C. R. Mecanique 344 (2016) 556–568

Contents lists available at ScienceDirect

Comptes Rendus Mecanique

www.sciencedirect.com

Large deflection and rotation of Timoshenko beams with frictional end supports under three-point bending

Dao-Kui Li [a], Xian-Fang Li [b,*]

[a] College of Aerospace Science and Engineering, National University of Defense Technology, Changsha 410073, PR China
[b] School of Civil Engineering, Central South University, Changsha 410075, PR China

ARTICLE INFO

Article history:
Received 9 December 2015
Accepted 30 January 2016
Available online 7 June 2016

Keywords:
Geometric nonlinearity
Timoshenko beam
Large deflection
Large rotation
Three-point bending
Frictional support

ABSTRACT

Three-point bending of a beam is studied based on the Timoshenko beam theory. Large deflection and large rotation of a beam resting on simple supports with friction are calculated for a concentrated force acting at the midspan. Using the Lagrangian kinematic relations, a system of non-linear differential equations are obtained for a prismatic shear-deformable Timoshenko beam. Exact solutions for the deflection, horizontal displacement, and rotation of cross-section are derived analytically. Two deflections of small and large scale exist under three-point bending. The solutions corresponding to linearized model coincide with the well-known solutions to the classical Timoshenko beams. Numerical calculations are carried out to show the effect of the important parameters such as shear rigidity of the beam and the coefficient of friction at the contact position between the beam and supports on the deflection. The load–deflection curves are graphically presented. A comparison of large deflections and large rotations with their classical counterparts and with experimental data is made. The obtained results are useful in safety design of linear and non-linear beams subject to three-point bending.

1. Introduction

Large deflection analysis of beams is of much significance in practice. Simple beam theories are based on the linear theories of geometry and materials of a beam. Numerical results based on these linear theories cannot be applied to large deflection predictions since they may lead to severe errors.

For Euler–Bernoulli beams, nonlinearity arising from the beam's geometry and from the materials has been studied extensively. Large deflection calculation of Euler–Bernoulli beams as a subject of research has a long history. So far, a large number of theoretical methods have been proposed to determine the large deflections of Euler–Bernoulli beams due to geometric and material nonlinearity. For example, for a simply-supported beam, elliptic integrals are applied to calculate large deflections for a centrally-loaded simply-supported beam (e.g., [1–3]). When a simply-supported beam is subjected to moment at ends, large deflections have been calculated in [4–6]. Large deflections of a simply-supported beam under both concentrated forces and uniformly distributed loading have been determined via various approaches such as shooting optimization technique [7], the minimum residual method [8], the integral approach [9], the Runge–Kutta–Felhberg method [10],

* Corresponding author. Tel.: +86 731 8816 7070; fax: +86 731 8557 1736.
E-mail address: xfli@csu.edu.cn (X.-F. Li).

http://dx.doi.org/10.1016/j.crme.2016.01.007
1631-0721/

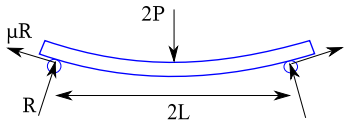

Fig. 1. Schematic of a centrally-loaded beam resting on simple supports under three-point bending.

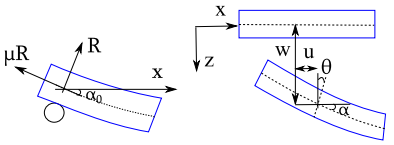

Fig. 2. An element to describe Lagrangian kinematic relationship.

etc. When subjected to a follower force, the large deflection analysis has been conducted by Shavartsman [11], Nallathambi et al. [12].

In addition to the above-stated geometric nonlinearity, large deflections owing to material nonlinearity also attract considerable attention of many researchers. For a class of non-linear beams, Lewis and Monasa [13,14] dealt with the large deflections of thin cantilever beams when subjected to a concentrated load and an end moment at the free end, respectively. The large deflections of a non-linear cantilever beam under combined loading were coped with in [15]. The large deflections of a non-linear cantilever beam with bimodulus have been investigated in [16]. Furthermore, Brojan et al. [17] calculated the large deflections of a non-prismatic slender and inextensible cantilever beam subjected to a concentrated moment at the free end. Kang and Li [18,19] calculated the large deflections of a cantilever beam made of functionally graded materials and obeying non-linear Ludwick stress–strain relations under a concentrated bending moment and a concentrated force. Borboni and De Santis [20] further studied the large deflections of an asymmetric Ludwick cantilever beam subjected to a horizontal force, a vertical force, and a bending torque at the free end.

Most of the above-mentioned researches are limited to Euler–Bernoulli beams. In other words, shear deformation of the cross-section of a beam is neglected or shear rigidity is assumed to be sufficiently large during the process of bending deformation. In fact, the effect of shear deformation is quite significant, especially for short beams. In fact, a substantial error in the effective elastic modulus results from shear deformation and the change in cross-section shape near the support contact positions and loading position from three-point bending tests of animal bones [21,22]. Even for nanoscale three-point bending tests, the contribution of shear deformation on the deflection and then on the stiffness of the nanotube deduced by the load–deflection relation is not negligible [23]. The influence of shear deformation along with scale parameters on the deflection of a nanobeam as well as the effective Young's modulus of the nanobeam has been analyzed [24,25]. If shear deformation is further taken into account, the classical linear Timoshenko beam theory accounts for the above phenomena. For large deflection analysis based on the Timoshenko beam theory, Li and Song [26] solved large thermal deflections of Timoshenko beams under transverse non-uniform temperature rise. Mohyeddin and Fereidoon [27] formulated a method for calculating large deflections of a beam under three-point bending. Li and Lee [28] analyzed the effect of the horizontal reaction force at the support position on the large deflection of short simply-supported Timoshenko beams subjected to general transverse loading. Batista [29] formulated Jacobi elliptic functions to determine large deflections of a Reissner's beam under three-point bending.

In this paper, a straight prismatic Timoshenko beam resting on simple supports is analyzed when subjected to a concentrated force at the midspan. An emphasis is placed on the effect of friction on the deflection. Using suitable boundary conditions, nonlinear governing equations are solved and an exact solution is determined. The effects of shear rigidity and the coefficient of friction between the beam and supports on the deflection are discussed.

2. Basic equations

Consider the bending of a straight prismatic Timoshenko beam of length $2L$ under a concentrated force $2P$ at the beam midspan $x = L$, as shown in Fig. 1. A Cartesian coordinate system is introduced such that the x- and z-axes are orientated along the neutral surface (axis) and perpendicular to the neutral surface (axis) downward, respectively. Using the Lagrangian description, kinematic relations for a prismatic Timoshenko beam can be represented as (see Fig. 2)

$$u^*(x,z) = u(x) - z\sin\theta \tag{1}$$

$$w^*(x,z) = w(x) - z(1-\cos\theta) \tag{2}$$

where $u^*(x,z)$ and $w^*(x,z)$ denote the displacement components at an arbitrary position in the beam along the x- and z-axes, respectively, $u(x)$ and $w(x)$ are the corresponding displacement components at the neutral axis, respectively, and θ represents the rotation of cross-section at the neutral axis. For Timoshenko beams, the rotation angle of cross-section does not coincide with the slope angle of the deflection, i.e. $\theta \neq \mathrm{d}w/\mathrm{d}x$, even for a small deformation. With these displacement components together with the rotation, one gets the axial strain and the shear strain as follows:

$$\varepsilon_{xx}(x,z) = \frac{\mathrm{d}u}{\mathrm{d}x} - z\kappa(x) \tag{3}$$

$$\gamma_{xz}(x,z) = \frac{\mathrm{d}w}{\mathrm{d}x} - \left(1 + z\frac{\mathrm{d}\theta}{\mathrm{d}x}\right)\sin\theta \tag{4}$$

respectively, where $\kappa(x)$ stands for curvature of the neutral axis, i.e.

$$\kappa(x) = \frac{\mathrm{d}\theta}{\mathrm{d}s} = \cos\theta\frac{\mathrm{d}\theta}{\mathrm{d}x} \tag{5}$$

It is noted that the relations (3)–(5) are identical to those in the classical treatment. However, the displacement components u^* and w^* are both dependent on z and applicable to a large rotation angle θ. If restricting θ to small values, we have $\sin\theta \approx \theta$ and $1 - \cos\theta \approx 0$. The above displacement components u^* and w^* reduce to the classical Timoshenko hypothesis, in which w^* is only dependent on x. For large deflection or large rotation of Timoshenko beams, in addition to the deflection and rotation of cross-section along with the horizontal displacement, geometric nonlinearity occurs and needs to be analyzed.

Based on the constitutive relationships for one-dimensional structures, we have

$$\sigma_{xx} = E\varepsilon_{xx} \tag{6}$$

$$\tau_{xz} = G\gamma_{xz} \tag{7}$$

where σ_{xx} and τ_{xz} are the axial stress and shear stress, respectively, E and G denote Young's modulus and shear modulus, respectively. It is worth noting that the stress–strain relations adopted here are still linear, rather than nonlinear. Actually, this paper only considers geometric nonlinearity, referring to large deflection accompanied with large rotation, not material nonlinearity.

3. Large deflection analysis

In order to determine the large deflections of a Timoshenko beam, it is natural to establish relationships between applied load and deformation variables. To this end, let us calculate axial force N, shear force Q, and bending moment M, through the following integrals

$$N = \int_A \sigma_{xx}\,\mathrm{d}A \tag{8}$$

$$Q = \int_A \tau_{xz}\,\mathrm{d}A \tag{9}$$

$$M = \int_A z\sigma_{xx}\,\mathrm{d}A \tag{10}$$

where A is the cross-sectional area. Inserting (6) and (7) in connection with (3) and (4) into (8)–(10) yields

$$N = EA\frac{\mathrm{d}u}{\mathrm{d}x} \tag{11}$$

$$Q = kGA\left(\frac{\mathrm{d}w}{\mathrm{d}x} - \sin\theta\right) \tag{12}$$

$$M = -EI\kappa(x) \tag{13}$$

where I is the moment of inertia of the cross-sectional area, and k is the shear correction coefficient.

Consider the bending of a simply supported beam subjected to a concentrated force at the beam midspan. The reaction forces at the supports are assumed to be normal to the beam surface posterior to bending deformation and frictional forces tangential to the surface of the bent beam are accompanied. Due to the symmetry of the problem we consider a half of the beam, the left-half portion, say.

Making use of balance of forces, we get

$$R\cos\alpha_0 + \mu R\sin\alpha_0 = P \tag{14}$$

where R is the reaction force at the support $x = 0$, α_0 is the slope angle of the deflection at the support $x = 0$, and μ is the coefficient of friction. Clearly, for the case of a small rotation angle α_0, we can approximate $\alpha_0 \approx 0$, and then $R \approx P$. It is worth emphasizing that here we treat the case of a large rotation angle α_0, which may reach 30 degrees or 80 degrees for some cases, as will be seen. Under such circumstances, we have the resultant axial and shear forces at an arbitrary cross-section

$$N = R\sin\alpha_0 - \mu R\cos\alpha_0 \tag{15}$$

$$Q = R\cos\alpha_0 + \mu R\sin\alpha_0 \tag{16}$$

Thus with the above results, if introducing a parameter β such that

$$\tan\beta = \mu \tag{17}$$

we further obtain

$$N = P\tan(\alpha_0 - \beta) \tag{18}$$

$$Q = P \tag{19}$$

$$M = Pw\tan(\alpha_0 - \beta) + Px \tag{20}$$

In the above, the internal bending moment contains two terms. The first term arises from the contribution of the horizontal axial force and the other from that of the vertical shear force. Note that a moment appears when the friction force μR is shifted from the contact position to the neutral surface of the beam and has been neglected since the beam depth is small enough.

Next, from (11)–(13) and (18)–(20), we get a system of differential equations as follows:

$$P\tan(\alpha_0 - \beta) = EA\frac{\mathrm{d}u}{\mathrm{d}x} \tag{21}$$

$$P = kGA\left(\frac{\mathrm{d}w}{\mathrm{d}x} - \sin\theta\right) \tag{22}$$

$$Pw\tan(\alpha_0 - \beta) + Px = -EI\kappa(x) \tag{23}$$

From (21) one easily finds

$$u = \frac{P}{EA}(x + C_1)\tan(\alpha_0 - \beta) \tag{24}$$

where C_1 is a constant, which can be determined from the midspan displacement condition, namely

$$u(L) = 0 \tag{25}$$

Accordingly, one has

$$u = \frac{P}{EA}(x - L)\tan(\alpha_0 - \beta) \tag{26}$$

Obviously, this function linearly depends on the local position. In the above derived expression for the horizontal displacement, the parameter α_0 is unknown for the time being, which will be determined in what follows.

For convenience of further analysis, we introduce dimensionless variables

$$W = \frac{w}{L}, \qquad \xi = \frac{x}{L} \tag{27}$$

$$p = \frac{PL^2}{EI}, \quad \psi = \frac{EI}{kGAL^2} \tag{28}$$

and rewrite (22) and (23) in a dimensionless form

$$p\,\psi = \frac{\mathrm{d}W}{\mathrm{d}\xi} - \sin\theta \tag{29}$$

$$p\,W\tan(\alpha_0 - \beta) + p\xi = -\cos\theta\frac{\mathrm{d}\theta}{\mathrm{d}\xi} \tag{30}$$

From the above two equations, we eliminate θ and obtain a second-order ordinary differential equation with an unknown parameter α_0

$$\frac{\mathrm{d}^2W}{\mathrm{d}\xi^2} + pW\tan(\alpha_0 - \beta) = -p\,\xi \tag{31}$$

As pointed out in [30], several possible choices on the boundary conditions for a clamped end can be selected. For the present problem, the corresponding boundary conditions are either

$$W(0) = 0, \qquad \left.\frac{\mathrm{d}W}{\mathrm{d}\xi}\right|_{\xi=1} = 0 \tag{32}$$

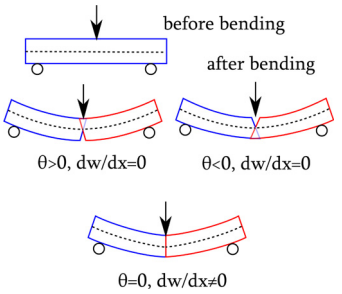

Fig. 3. Diagram of a comparison of the boundary conditions on the slope angle of the deflection and rotation angle of cross-section at the midspan of a centrally-loaded simply-supported beam.

or

$$W(0)=0, \qquad \theta(1)=0 \tag{33}$$

However, there is an essential difference for two choices. For the former, the physical meaning is clear for Euler–Bernoulli beams. For Timoshenko beams, the latter seems to be more reasonable since, by virtue of (22), the corresponding rotation of cross-section at the beam midspan $\theta(1)\neq 0$ if adopting (32) results is incompatible with or contradictory to the symmetry of the problem. This can be seen from an illustrative diagram (Fig. 3). Due to this reason, in this paper we use the boundary conditions in (33).

First, in the case of $\alpha_0=\beta$, this case is quite simple and the solution to (31) subjected to the boundary conditions in (33) is readily derived as

$$W=\frac{1}{6}p\xi\left[3(1+2\psi)-\xi^2\right] \tag{34}$$

$$\theta=\sin^{-1}\left[\frac{1}{2}p\left(1-\xi^2\right)\right] \tag{35}$$

If restricting the rotation of the cross-section θ in order for it to be small, we have $\sin\theta\approx\theta$, and the classical results for the bending of Timoshenko beams are recovered from the above [30]. This is not surprising, since the moment resulting from the horizontal force corresponding to the first term at the left-hand side of (30) disappears in the case where $\alpha_0=\beta$.

Next let us consider another case in which $\alpha_0\neq\beta$. For instance, smooth contact at end supports belongs to this case. Solving Eq. (31), because of $\alpha_0>\beta$, one has

$$W=C_2\cos\left[\sqrt{p\tan(\alpha_0-\beta)}\xi\right]+C_3\sin\left[\sqrt{p\tan(\alpha_0-\beta)}\xi\right]-\frac{\xi}{\tan(\alpha_0-\beta)} \tag{36}$$

where C_2 and C_3 are still unknown, which can be determined through appropriate boundary conditions.

Since the expression for the deflection contains an unknown parameter α_0 and two unknown constants C_2 and C_3, we need three conditions to determine them. Applying the first condition in (33), one gets $C_2=0$. With this result in mind, using (29) we have

$$\sin\theta=C_3\sqrt{p\tan(\alpha_0-\beta)}\cos\left[\sqrt{p\tan(\alpha_0-\beta)}\xi\right]-\frac{1}{\tan(\alpha_0-\beta)}-p\psi \tag{37}$$

Next the second condition in (33) permits us to obtain

$$C_3=\left[\psi+\frac{1}{p\tan(\alpha_0-\beta)}\right]\frac{p}{\sqrt{p\tan(\alpha_0-\beta)}\cos\sqrt{p\tan(\alpha_0-\beta)}} \tag{38}$$

and the desired deflection is then obtained as

$$W=\left[\psi+\frac{1}{p\tan(\alpha_0-\beta)}\right]\frac{p\sin\left[\sqrt{p\tan(\alpha_0-\beta)}\xi\right]}{\sqrt{p\tan(\alpha_0-\beta)}\cos\sqrt{p\tan(\alpha_0-\beta)}}-\frac{\xi}{\tan(\alpha_0-\beta)} \tag{39}$$

To determine α_0, we differentiate W with respect to ξ, leading to

$$\frac{\mathrm{d}W}{\mathrm{d}\xi}=\left[\psi+\frac{1}{p\tan(\alpha_0-\beta)}\right]\frac{p\cos\left[\sqrt{p\tan(\alpha_0-\beta)}\xi\right]}{\cos\sqrt{p\tan(\alpha_0-\beta)}}-\frac{1}{\tan(\alpha_0-\beta)} \tag{40}$$

According to the definition of α_0, by setting $\xi=0$ in the above expression (40), we have $\mathrm{d}W/\mathrm{d}\xi=\tan\alpha_0$, which is a condition to determine the end slope angle. Note that the end slope angle is not equal to the rotation angle of the cross-section for Timoshenko beams. Thus

$$\tan\alpha_0 = \left[p\psi + \frac{1}{\tan(\alpha_0-\beta)}\right]\left[\frac{1}{\cos\sqrt{p\tan(\alpha_0-\beta)}} - 1\right] \tag{41}$$

Eq. (41) is a nonlinear equation in α_0. A further simplification may be made by introducing a parameter

$$s = \tan(\alpha_0 - \beta) \tag{42}$$

Considering (17), we have

$$\tan\alpha_0 = \frac{s+\mu}{1-s\mu} \tag{43}$$

and after some algebra, Eq. (41) becomes the following form

$$\cos\sqrt{p\,s} = \left[1 + \frac{s(s+\mu)}{(1-s\,\mu)(1+s\,p\,\psi)}\right]^{-1} \tag{44}$$

Consequently, the determination of α_0 is transformed to seek a root of transcendental Eq. (44). Its solution can be numerically determined. From the above, taking into account $\mu > 0$ and $1 - s\,\mu > 0$, there are two positive roots for certain positive values of p and ψ. Similar to [31], the deflection corresponding to the smaller one is called the small-scale deflection, and that to the larger one is called the large-scale deflection. Once two roots s_0 of (44) are determined, the end slope angle α_0 is given through

$$\alpha_0 = \tan^{-1}\mu + \tan^{-1}s_0 \tag{45}$$

Therefore, the large deflection of a Timoshenko beam is obtained as (39) and the rotation θ of cross-section is given by

$$\theta = \sin^{-1}\left\{\left[p\,\psi + \frac{1}{\tan(\alpha_0-\beta)}\right]\left[\frac{\cos\left[\sqrt{p\tan(\alpha_0-\beta)}\,\xi\right]}{\cos\sqrt{p\tan(\alpha_0-\beta)}} - 1\right]\right\} \tag{46}$$

In this case, at the midspan of the beam, we find

$$\left.\frac{\mathrm{d}W}{\mathrm{d}\xi}\right|_{\xi=1} = p\,\psi \tag{47}$$

This implies that at the midspan, the slope of the deflection does not vanish, but the rotation of cross-section vanishes, which means that the cross-section at the beam midspan does not rotate, while other cross-sections rotate and deviate away from the original position, as shown in Fig. 3. If the shear rigidity is sufficiently large, or $\psi \to 0$, thus the slope of deflection reduces to zero. This actually corresponds to the Euler–Bernoulli hypothesis. For the latter, $\theta = \mathrm{d}W/\mathrm{d}\xi$, and both vanish at the midspan.

Now we turn our attention to having a look at $\mathrm{d}^2W/\mathrm{d}\xi^2$. By performing the second derivative of W, we get

$$\frac{\mathrm{d}^2W}{\mathrm{d}\xi^2} = -[p\,\psi\tan(\alpha_0-\beta)+1]\sqrt{\frac{p}{\tan(\alpha_0-\beta)}}\frac{\sin\left[\sqrt{p\tan(\alpha_0-\beta)}\,\xi\right]}{\cos\sqrt{p\tan(\alpha_0-\beta)}} \tag{48}$$

This is to say that $\mathrm{d}^2W/\mathrm{d}\xi^2$ indeed vanishes at the end supports, as expected.

In the following, we consider two special cases.

3.1. Frictionless end supports

If contact at simple supports is frictionless, meaning $\mu = 0$, or $\beta = 0$, one has the deflection and rotation as

$$W = \left(p\,\psi + \frac{1}{s_0}\right)\frac{\sin\left[\sqrt{p\,s_0}\xi\right]}{\sqrt{ps_0}\cos\sqrt{ps_0}} - \frac{\xi}{s_0} \tag{49}$$

$$\theta = \sin^{-1}\left\{\left[p\psi + \frac{1}{s_0}\right]\left[\frac{\cos\left(\sqrt{ps_0}\xi\right)}{\cos\sqrt{ps_0}} - 1\right]\right\} \tag{50}$$

where s_0 is the smallest positive root of the following equation

$$\cos\sqrt{ps} = \left(1 + \frac{s^2}{1+sp\psi}\right)^{-1} \tag{51}$$

In particular, for $\psi \to 0$, equivalent to an Euler–Bernoulli beam, we have

$$\cos\sqrt{p\,s} = \frac{1}{1+s^2} \tag{52}$$

Table 1
The end slope angle α_0 (in degrees) for frictionless end supports.

ψ	p											
	0.001	0.1	0.2	0.3	0.4	0.5	0.6	0.7	0.8	0.9	1	1.1
0	0.029	2.868	5.759	8.694	11.703	14.819	18.088	21.578	25.402	29.773	35.238	46.037
	89.977	87.674	85.327	82.934	80.467	77.894	75.167	72.219	68.937	65.108	60.185	49.928
0.1	0.029	2.870	5.770	8.735	11.802	15.021	18.460	22.223	26.493	31.669	39.202	–
	89.977	87.673	85.317	82.900	80.384	77.722	74.847	71.657	67.971	63.390	56.467	–
0.2	0.029	2.871	5.782	8.775	11.902	15.228	18.848	22.912	27.706	33.969	–	–
	89.977	87.672	85.307	82.865	80.299	77.545	74.512	71.055	66.890	61.284	–	–

In this case, the maximum deflection occurs at $\xi = 1$, namely

$$W(1) = p\,\psi\frac{\tan\sqrt{p\,s_0}}{\sqrt{p\,s_0}} + \frac{1}{s_0}\left(\frac{\tan\sqrt{p\,s_0}}{\sqrt{p\,s_0}} - 1\right) \tag{53}$$

3.2. Linearized model

By linearizing the theory presented above, one obtains the classical (linear) Timoshenko beam theory. To this end, large rotation collapses to small rotation, i.e.

$$\sin\theta \approx \theta, \quad \cos\theta \approx 1 \tag{54}$$

Moreover, neglecting the horizontal displacement and horizontal force, from (22) and (23), we get

$$p\,\psi = \frac{\mathrm{d}W}{\mathrm{d}\xi} - \theta \tag{55}$$

$$p\,\xi = -\frac{\mathrm{d}\theta}{\mathrm{d}\xi} \tag{56}$$

in terms of the introduced dimensionless variables. In fact, since the first term in the left-hand side of (30) describes bending moment caused by the horizontal force, for small deflection, $W << 1$, we neglect the contribution of the bending moment caused by the horizontal force. In other words, at simply supported ends, the reaction forces at the contact position between the beam and the support ends are assumed to be vertical, rather than normal to the beam surface after the bending deformation. This coincides with the conventional treatment for small deflection analysis. Under such circumstances, we integrate (55) and (56) to obtain

$$W = p\,\psi\,\xi + p\left(\frac{1}{2}\xi - \frac{1}{6}\xi^3\right), \quad 0 \le \xi \le 1 \tag{57}$$

$$\theta = \frac{1}{2}\,p\left(1 - \xi^2\right), \quad 0 \le \xi \le 1 \tag{58}$$

If setting $\xi = 1$, the rotation of cross-section at the midspan clearly vanishes, as expected. In addition, we get the maximum deflection at the midspan as

$$w(L) = \frac{PL^3}{3EI} + \frac{PL}{kGA} \tag{59}$$

Keeping the beam span being $2L$ and concentrated force being $2P$ in mind, it is viewed that the above results are in exact agreement with those derived in [30]. Of course, if further imposing $kGA \to \infty$, the above results reduce to those for Euler–Bernoulli beams. This is readily understood since $\mathrm{d}W/\mathrm{d}\xi = \theta$ can be derived in this case. Therefore, for sufficient large shear rigidity, the rotation of cross-section coincides with the slope angle of the deflection, implying that Timoshenko beams reduce to Euler–Bernoulli beams, as expected.

4. Numerical results and discussion

In this section, numerical results are presented to show the dependence of large deflections on several parameters of interest.

4.1. End slope angle

We first numerically determine the end slope angle via (45) where s_0 is the root of Eq. (44). When the end supports are frictionless, the end slope angle satisfies (51). Calculated numerical results of the end slope angle are tabulated in Table 1. From Table 1, it is seen that two sets of the end slope angle can be sought for $\psi = 0$ if $p < 1.1025$. This indicates that

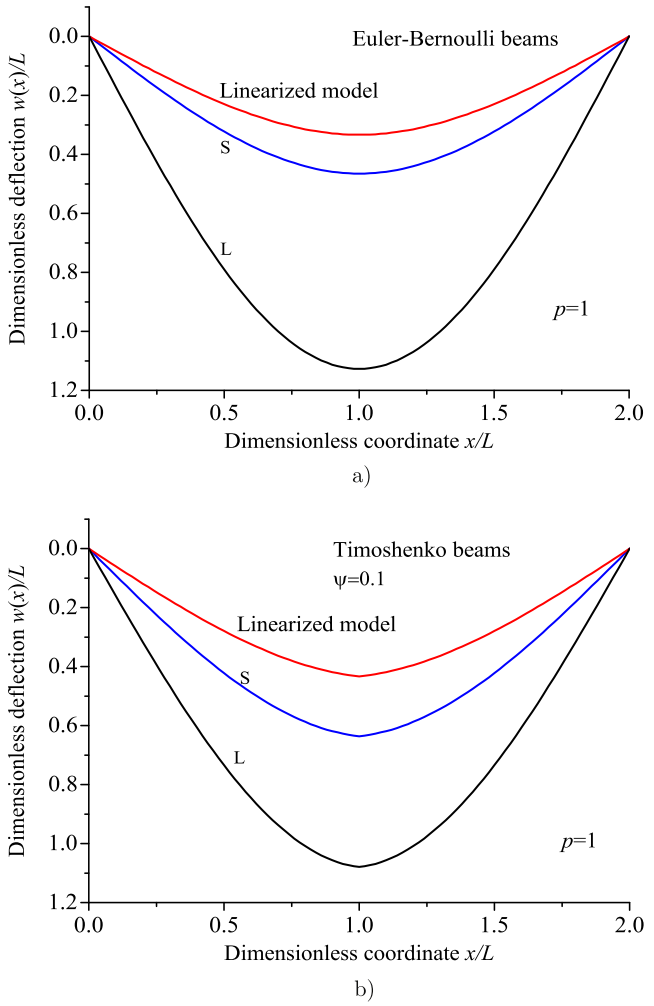

Fig. 4. A comparison of the deflection for a centrally-loaded simply-supported beam with its linearized model with $p = 1$, $\mu = 0$, the curve marked with label S means the small scale deflection and that with L means the large scale deflection; a) Euler–Bernoulli beams, b) Timoshenko beams with $\psi = 0.1$.

there exist two distinct deflections, a small-scale deflection corresponding to a small end slope angle and a large-scale deflection to a large end slope angle. In particular, for $p = 0.1$, we find that $\alpha_0 = 2.759°$ or $\alpha_0 = 87.674°$. For the former case, the bending shape is almost close to that of the linearized model, whereas for the latter case, the deformed beam at the supports is nearly normal to the beam prior to deformation, and the midspan deflection has a very large value. In this case, the shape of the beam after deformation looks like the letter U, which has been observed in experiment [3]. For $p = 1$, we depict the small- and large-scale deflections marked with labels S and L, which correspond to end slope angles about 35° and 60°, respectively, for Euler–Bernoulli and Timoshenko beams in Fig. 4(a,b). These angles correspond no longer to a small rotation, but to a large rotation. Meanwhile, the deflections of their linearized models are also demonstrated in Fig. 4(a,b) for contrast. From Table 1, we find that for given values of ψ, the end slope angle α_0 becomes larger with the concentrated force P_0 rising, as expected. However, for $\psi = 0.1$, the end slope angle does not exist when p is chosen larger than 1.1042. A similar phenomenon takes place for $\psi = 0.2$, and a suitable range of p values becomes smaller.

4.2. Large deflection

Once the end slope angle α_0 is determined, large deflections are easily obtained. Consider a centrally-loaded simply-supported beam with frictionless contact, a comparison of the large deflection of Timoshenko and Euler–Bernoulli beams with the deflection of the linearized models (i.e. the classical deflection) is made for $p = 1, \mu = 0$ (see Fig. 4(a,b)). Since Euler–Bernoulli beams neglect the effect of shear deformation, in calculations we choose $\psi = 0$, while for Timoshenko beams we choose $\psi = 0.1$. From (28), with $G = E/2(1+\nu)$, the parameter $\psi = 2(1+\nu) I/kAL^2$ takes $3I/AL^2$ if $\nu = 0.3$ and $k = 5(1+\nu)/(6+5\nu)$, thus the value of ψ is about 0.1 for a beam of square cross-section with aspect ratio $2L/a = 3.16$ (a: side length) or circular cross-section with $2L/D = 2.78$ (D: diameter). We find that the deflection of the latter is larger than that of the former, which is evident for the classical case (59). On the other hand, since there exist the small and

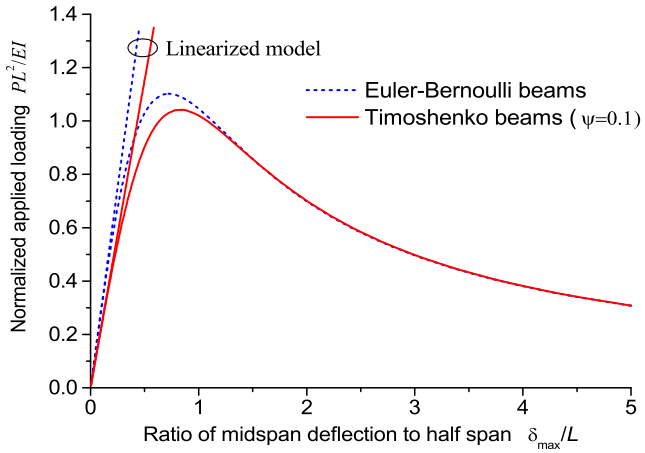

Fig. 5. Dimensionless applied loading versus the ratio of the midspan deflection to the half span length.

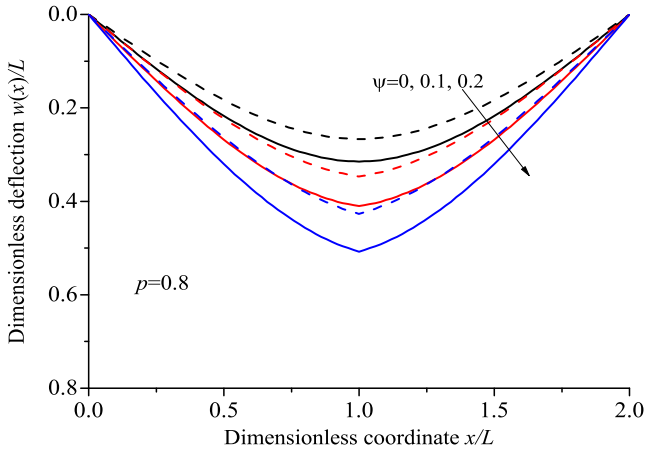

Fig. 6. Bending shapes of a centrally-loaded simply-supported beam for various values of shear rigidity with $p = 0.8$, $\mu = 0$, where solid lines denote the small scale deflection curves and dashed lines denote deflection curves of the corresponding linearized model.

large scale deflection curves corresponding to small and large end slope angles, respectively, they are labeled with S and L, respectively. From Fig. 4, one views that the numerical results of both small-scale and large-scale deflections are always greater than those of the deflection based on the corresponding classical theories. This characteristic is in agreement with that based on other approaches [1,3]. Such two equilibrium configurations for a given applied loading are a unified characteristic, irrespective of the applied end moment [6] or the concentrated force [1,3]. Generally speaking, the small-scale deflection is a stable equilibrium configuration, while the large scale deflection is an unstable equilibrium configuration, since further increase in deflection/rotation in this case requires no increment of applied loading.

In addition, by a careful inspection on Fig. 4, we find that the deflection curves at the midspan are smooth for Euler–Bernoulli beams, and not smooth for Timoshenko beams. It is attributed to the fact that the rotation of cross-section just vanishes at the midspan, but the slope of the deflection does not vanish, coinciding with the symmetry of the problem (see Fig. 3). Thus the deflection has a nonsmooth inflexion point at the midspan for Timoshenko beams. Fig. 5 shows the dimensionless maximum deflection at the midspan of the beam against dimensionless applied loading for Euler–Bernoulli and Timoshenko beams as well as their linearized models.

4.3. Effect of shear rigidity

The effect of shear deformation or shear rigidity on deflection is examined for a Timoshenko beam under three-point bending. The small scale deflections of a centrally-loaded simply-supported beam under three-point bending with $p = 0.8$, $\mu = 0$, $\psi = 0, 0.1, 0.2$ are presented in Fig. 6. The large-scale deflections are not depicted in Fig. 6. For comparison, we also display the deflection variation when using the linearized model, i.e. the deflection of the classical Timoshenko beam theory. Note that Euler–Bernoulli beams correspond to the case where $\psi = 0$. Clearly, consideration of shear deformation or shear rigidity gives rise to a further increase in the deflection. This trend is in agreement with that using the linearized theory. In fact, this case can be directly seen from (59), since consideration of shear deformation leads to an increase in deflection.

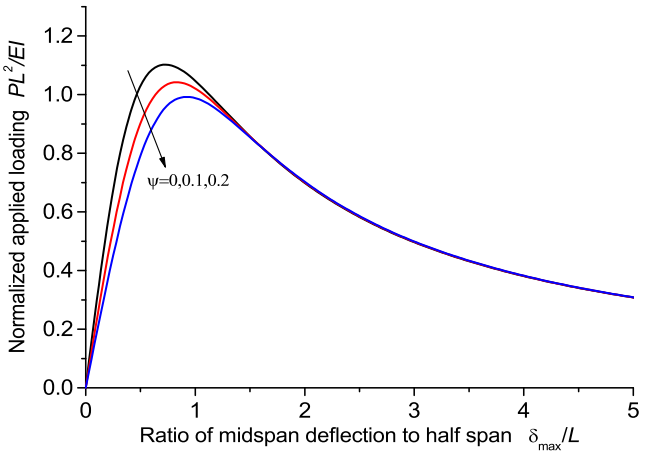

Fig. 7. Effect of shear rigidity on the ratio of the midspan deflection to the half span length as a function of dimensionless applied loading.

Table 2
Midspan deflection of a simply-supported beam under three-point bending for $\mu = 0$.

p	Linearized model	Present model		[27]	[31]
		$\psi = 0$	$\psi = 0.1$		
0.125	0.041 7	0.0418	0.0543	0.0410	0.0419
0.25	0.083 3	0.0844	0.1097	0.0844	0.0849
0.375	0.1250	0.1287	0.1672	0.1287	0.1306
0.5	0.166 6	0.1760	0.2285	0.1760	0.1811
0.625	0.208 3	0.2279	0.2959	0.2279	0.2411
0.75	0.25	0.2874	0.3740	0.2874	0.3242
0.834	0.278	0.3345	0.4370	0.3345	0.478
0.875	0.291 7	0.3607	0.4729	0.3607	–
1	0.333 3	0.4653	–	0.465 2	–
1.1025	0.367 5	0.7189	–	0.718 9	–

Table 3
Applied load estimation for given midspan deflection with $\mu = 0$.

$W(1)$	Linearized model		Present model		[3]	[32]
	$\psi = 0$	$\psi = 0.1$	$\psi = 0$	$\psi = 0.1$		
0.1	0.3	0.2308	0.296	0.245	0.2924	0.295
0.2	0.6	0.4615	0.560	0.443	0.5422	0.55
0.3	0.9	0.6923	0.774	0.632	0.7196	0.735
0.4	1.2	0.9231	0.929	0.789	0.8134	0.81

To show the small- and large-scale deflections for different applied loading, the midspan deflection is only presented in Fig. 7 for several values of ψ against dimensionless applied loadings. From Fig. 7, two midspan deflections correspond to each applied loading. Moreover, with shear rigidity rising, the midspan deflection has a slight increase. This implies that when shear deformation is taken into account, the small-scale deflection, which lies in the left-hand portion of the peak value of the corresponding curve becomes larger under the same loading. Nevertheless, for large-scale deflections lying the right-hand portion of the peak value, we find that they almost overlap for larger deflections under normalized applied loading less than about 0.9.

Here, we give a comparison of our numerical results of the midspan deflection of a simply-supported beam under three-point bending for $\mu = 0$ with the experimental data as well as previous theoretical results based on the Euler–Bernoulli beam theory in Tables 2 and 3. From these tables, numerical results are in satisfactory agreement with experimental data and theoretical results based on other approaches.

4.4. Effect of friction

Finally, the effect of friction at the contact position on the deflection is examined. For Euler–Bernoulli beams and Timoshenko beams, the variation of the small scale deflection is illustrated in Fig. 8(a,b), respectively. In calculations, the applied concentrated force is chosen as $p = 1$ and shear rigidity is taken such that $\psi = 0.1$. From Fig. 8, it is seen that the presence of friction results in a decrease in the deflection. In other words, if friction at the contact position between the beam and supports is considered, the beam appears to become stiffer. This can be explained as follows. When friction exists at the

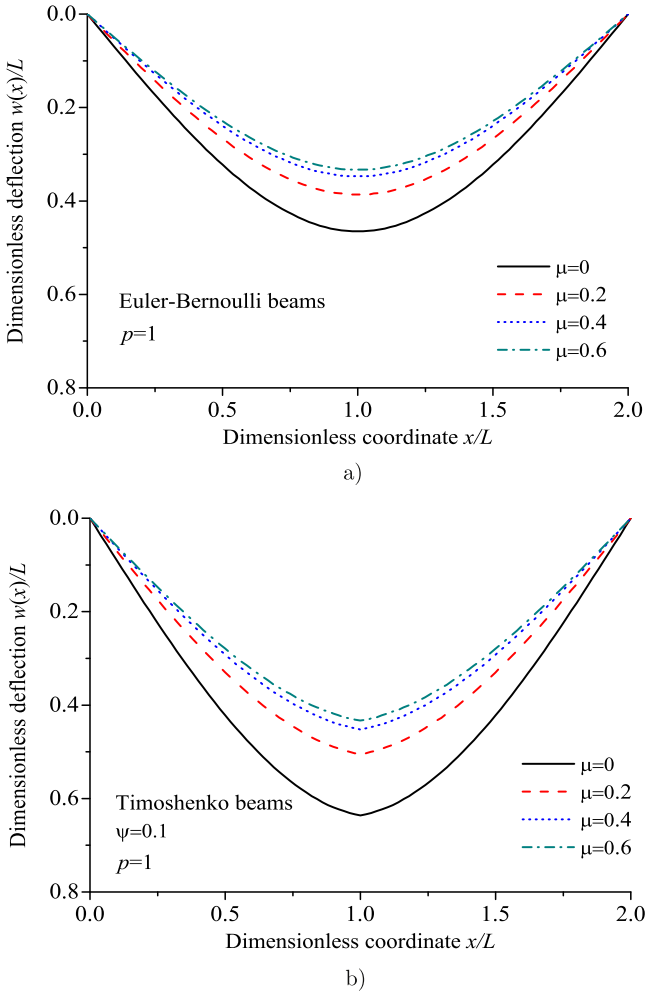

Fig. 8. Bending shapes of the small scale deflection of a centrally-loaded simply-supported beam with $p = 1$ for various values of the coefficient of friction; a) Euler–Bernoulli beams, b) Timoshenko beams with $\psi = 0.1$.

contact position, as if there are two horizontal forces to pull oppositely the beam tight along its axial direction, thus the beam is more difficult to bend. In the absence of friction, the beam readily bends under transverse forces.

At the midspan of a centrally-loaded simply-supported beam, the deflection arrives at its maximum. To show the variation of the small- and large-scale deflection against applied loading, the ratio of the midspan deflection to the half span for different applied loadings is displayed for Euler–Bernoulli beams (dashed lines) and Timoshenko beams (solid lines) for various values of the coefficient of friction in Fig. 9. From Fig. 9, when the coefficient of friction becomes larger, the applied loading reaches a larger peak value, which indicates that the deflections of the linearized models are closer to small-scale deflections. Therefore, the linearized models are reasonable for large values of the coefficients of friction.

5. Conclusions

The large deflections of a simply-supported beam under three-point bending were investigated using the Timoshenko beam theory. Based on the nonlinear kinematic relationships of Timoshenko beams, governing equations were derived for a beam resting on simple supports with the emphasis on the added feature of friction. The classical results can be recovered from the present ones when linearized models are used. The obtained results are useful in safety design of linear and nonlinear beams. Some conclusions are drawn as follows:

- expressions for large deflection and large cross-sectional rotation of a simply-supported beam under three-point bending were derived;
- the presence of friction gives rise to a decrease in the deflection of a simply-supported beam, as if the beam becomes stiffer;

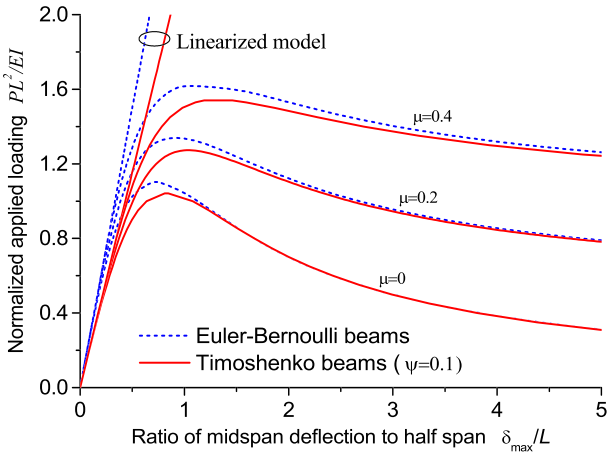

Fig. 9. Effect of the coefficient of friction on the ratio of the midspan deflection to the half span length as a function of dimensionless applied loading.

- consideration of shear deformation or shear rigidity increases the deflection, as compared to Euler–Bernoulli beams, irrespective of large or small deflection analysis;
- the deflections under large deflection/rotation assumption is greater than those based on the classical linear theory for a simply-supporter beam.

Acknowledgement

This work was supported by the National Natural Science Foundation of China (No. 11472003).

References

[1] C.M. Wang, K.Y. Lam, X.Q. He, S. Chucheepsakul, Large deflections of an end supported beam subjected to a point load, Int. J. Non-Linear Mech. 32 (1997) 63–72.
[2] H. Tari, On the parametric large deflection study of Euler–Bernoulli cantilever beams subjected to combined tip point loading, Int. J. Non-Linear Mech. 49 (2013) 90–99.
[3] M. Batista, Large deflections of a beam subject to three-point bending, Int. J. Non-Linear Mech. 69 (2015) 84–92.
[4] P. Seide, Large deflections of a simply supported beam subjected to moment at one end, J. Appl. Mech. 51 (1984) 519–525.
[5] S. Chucheepsakul, S. Buncharoen, C.M. Wang, Large deflection of beams under moment gradient, J. Eng. Mech. 120 (1994) 1848–1860.
[6] S. Chucheepsakul, S. Buncharoen, T. Huang, Elastica of simple variable-arc-length beam subjected to end moment, J. Eng. Mech. 121 (1995) 767–772.
[7] C.M. Wang, S. Kitipornchai, Shooting optimization technique for large deflection analysis of structural members, Eng. Struct. 14 (1992) 231–240.
[8] M. Dado, S. Al-Sadder, A new technique for large deflection analysis of non-prismatic cantilever beams, Mech. Res. Commun. 32 (2005) 692–703.
[9] L. Chen, An integral approach for large deflection cantilever beams, Int. J. Non-Linear Mech. 45 (2010) 301–305.
[10] T. Belendez, M. Perez-Polo, C. Neipp, A. Belendez, Numerical and experimental analysis of large deflections of cantilever beams under a combined load, Phys. Scr. T 118 (2005) 61–65.
[11] B.S. Shavartsman, Large deflections of cantilever beam subjected to a follower force, J. Sound Vib. 304 (2007) 969–973.
[12] A.K. Nallathambi, C.L. Rao, S.M. Srinivasan, Large deflection of constant curvature cantilever beam under follower load, Int. J. Mech. Sci. 52 (2010) 440–445.
[13] G. Lewis, F. Monasa, Large deflections of cantilever beams of nonlinear materials, Compos. Struct. 14 (1981) 357–360.
[14] G. Lewis, F. Monasa, Large deflections of cantilever beams of nonlinear materials of the Ludwick type subjected to an end moment, Int. J. Non-Linear Mech. 17 (1982) 1–6.
[15] K. Lee, Large deflections of cantilever beams of nonlinear elastic material under a combined loading, Int. J. Non-Linear Mech. 37 (2002) 439–443.
[16] C. Baykara, U. Guven, I. Bayer, Large deflections of a cantilever beam of nonlinear bimodulus material subjected to an end moment, J. Reinf. Plast. Compos. 24 (2005) 1321–1326.
[17] M. Brojan, T. Videnic, F. Kosel, Large deflections of nonlinearly elastic non-prismatic cantilever beams made from materials obeying the generalized Ludwick constitutive law, Meccanica 44 (2009) 733–739.
[18] Y.-A. Kang, X.-F. Li, Large deflections of a non-linear cantilever functionally graded beam, J. Reinf. Plast. Compos. 29 (2010) 1761–1774.
[19] Y.-A. Kang, X.-F. Li, Bending of functionally graded cantilever beam with power-law non-linearity subjected to an end force, Int. J. Non-Linear Mech. 44 (2009) 696–703.
[20] A. Borboni, D. De Santis, Large deflection of a non-linear, elastic, asymmetric Ludwick cantilever beam subjected to horizontal force, vertical force and bending torque at the free end, Meccanica 49 (2014) 1327–1336.
[21] J.L. Schriefer, A.G. Robling, S.J. Warden, A.J. Fournier, J.J. Mason, C.H. Turner, A comparison of mechanical properties derived from multiple skeletal sites in mice, J. Biomech. 38 (2005) 467–475.
[22] L.C. Kourtis, D.R. Carter, G.S. Beaupre, Improving the estimate of the effective elastic modulus derived from three-point bending tests of long bones, Ann. Biomed. Eng. 42 (2014) 1773–1780.
[23] B. Lecouvet, J. Horion, C. D'Haese, C. Bailly, B. Nysten, Elastic modulus of halloysite nanotubes, Nanotechnology 24 (2013) 105704.
[24] X.-F. Li, H. Zhang, K.Y. Lee, Dependence of Young's modulus of nanowires on surface effect, Int. J. Mech. Sci. 81 (2014) 120–125.
[25] X.-L. Peng, X.-F. Li, G.-J. Tang, Z.-B. Shen, Effect of scale parameter on the deflection of a nonlocal beam and application to energy release rate of a crack, Z. Angew. Math. Mech. 95 (2015) 1428–1438.
[26] S. Li, X. Song, Large thermal deflections of Timoshenko beams under transversely non-uniform temperature rise, Mech. Res. Commun. 33 (2006) 84–92.

[27] A. Mohyeddin, A. Fereidoon, An analytical solution for the large deflection problem of Timoshenko beams under three-point bending, Int. J. Mech. Sci. 78 (2014) 135–139.
[28] X.-F. Li, K.Y. Lee, Effect of horizontal reaction force on the deflection of short simply-supported beams under transverse loading, Int. J. Mech. Sci. 99 (2015) 121–129.
[29] M. Batista, Analytical solution for large deflection of Reissner's beam on two supports subjected to central concentrated force, Int. J. Mech. Sci. 107 (2016) 13–20.
[30] J.M. Gere, S.P. Timoshenko, Mechanics of Materials, 4th ed., PWS Pub. Co., Boston, 1997.
[31] A. Ohtsuki, An analysis of large deflections in a symmetrical three-point bending of beam, Bull. JSME 29 (1986) 1988–1995.
[32] D.C. West, Flexure testing of plastics, Exp. Mech. 21 (1964) 185–190.